HHS Public Access

Author manuscript

Calcif Tissue Int. Author manuscript; available in PMC 2020 April 16.

Published in final edited form as:

Calcif Tissue Int. 2019 December ; 105(6): 660–669. doi:10.1007/s00223-019-00603-3.

Substrate strain mitigates effects of β-aminopropionitrile-induced reduction in enzymatic crosslinking

Silvia P. Canelón[1], **Joseph M. Wallace**[2,3,#a,*]

[1]Weldon School of Biomedical Engineering, Purdue University, West Lafayette, Indiana, United States of America

[2]Department of Biomedical Engineering, Indiana University-Purdue University at Indianapolis, Indianapolis, Indiana, United States of America

[3]Department of Orthopaedic Surgery, Indiana University School of Medicine, Indianapolis, Indiana, United States of America

Abstract

Enzymatic crosslinks stabilize type I collagen and are catalyzed by lysyl oxidase (LOX), a step interrupted through β-aminopropionitrile (BAPN) exposure. This study evaluated dose-dependent effects of BAPN on osteoblast gene expression of type I collagen, LOX, and genes associated with crosslink formation. The second objective was to characterize collagen produced *in vitro* after exposure to BAPN, and to explore changes to collagen properties under continuous cyclical substrate strain.

To evaluate dose-dependent effects, osteoblasts were exposed to a range of BAPN dosages (0–10 mM) for gene expression analysis and cell proliferation. Results showed significant upregulation of *BMP-1*, *POST*, and *COL1A1*and change in cell proliferation. Results also showed while the gene encoding LOX was unaffected by BAPN treatment, other genes related to LOX activation and matrix production were upregulated.

For the loading study, the combined effects of BAPN and mechanical loading were assessed. Gene expression was quantified, atomic force microscopy was used to extract elastic properties of the collagen matrix, and Fourier Transform infrared spectroscopy was used to assess collagen secondary structure for enzymatic crosslinking analysis. BAPN upregulated *BMP-1* in static samples and BAPN combined with mechanical loading downregulated *LOX* when compared to control-static samples. Results showed a higher indentation modulus in BAPN-loaded samples compared to control-loaded samples. Loading increased the mature to immature crosslink ratios in control samples, and BAPN increased the height ratio in static samples.

In summary, effects of BAPN (upregulation of genes involved in crosslinking, mature/immature crosslinking ratios, upward trend in collagen elasticity) were mitigated by mechanical loading.

[*]Corresponding author: jmwalla@iupui.edu (J.M. Wallace).

[#a]Current Address: Department of Biomedical Engineering, Indiana University-Purdue University at Indianapolis, Indianapolis, Indiana, United States of America

Keywords

Osteoblast; collagen; indentation; BAPN; FTIR

Introduction

As a composite material, bone is made up of an inorganic hydroxyapatite mineral phase, a proteinaceous organic phase, and water. Type I collagen is the most abundant protein in the human body[1] and makes up 90% of the organic phase. Hydroxyapatite and collagen both contribute to bone mechanical properties: hydroxyapatite provides compressive strength and stiffness while collagen provides tensile strength and ductility [2–4]. Changes in either phase can impact bulk mechanical properties of the tissue and bone structure and can compromise structural and functional integrity.

Mature osteoblasts are responsible for synthesizing type I collagen in bone as a right-handed helical structure formed from three polypeptide chains of amino acids. Post-translationally, collagen fibrils are stabilized within their staggered array by intramolecular and intermolecular crosslinks [5–7]. Enzymatic crosslinks are initiated by the lysyl oxidase (LOX) enzyme and eventually form covalent chemical crosslinks between collagen molecules and fibrils.[6–8] Crosslink synthesis can be limited by compounds such as penicillamine and β-aminopropionitrile (BAPN), resulting in a crosslink deficiency which characterizes a disease known as lathyrism [9–11].

The ability of LOX to initiate enzymatic crosslinking also depends on direct or indirect interactions with other connective tissue proteins including bone morphogenic protein-1 (BMP-1), periostin (POST), and fibronectin [12–14]. LOX is synthesized as an inactive precursor, pro-LOX, and activated through propeptide proteolytic cleavage carried out by BMP-1. Maruhashi *et al.* found POST binds to BMP-1, enhances proteolytic cleavage of pro-LOX, and promotes the deposition of BMP-1 onto fibronectin in the extracellular matrix. In addition, their results suggest increased interactions between POST and fibronectin lead to increased enzymatic crosslinking [13]. These relationships are further complicated by interactions with fibronectin which have the potential to impact the structure and function of type I collagen (Fig. 1).

In addition to synthesizing collagen, osteoblasts also interact with osteoclasts and osteocytes to carry out bone modeling and remodeling processes in response to their mechanical environment [15]. Because of this role in bone development and maintenance, it is important to examine the osteoblast response to mechanical loading, and its effects on structural, biochemical, and mechanical properties of the secreted collagen matrix. Exercise has been found to have positive effects on bone structure and strength [16, 17] and mechanical loading of diseased bone has been shown to have compensatory effects on collagen properties in the context of BAPN-induced lathyrism [18, 19]. The effects of mechanical loading on the properties of collagen produced *in vitro* by osteoblasts have yet to be explored, much less characterized.

While BAPN has been shown to modify nanoscale properties, morphology, and crosslinking of type I collagen produced by osteoblasts *in vitro* [20], knowledge of its direct effects on the osteoblast response is limited [21–23]. BAPN also has not been evaluated for its effect on collagen mechanical properties nor has mechanical loading been explored for its potential compensatory effect on diseased collagen. Finally, BAPN provides an opportunity to take a mechanistic approach to understanding the effect of enzymatic crosslink inhibition on type I collagen properties. The purpose of this study was to expose osteoblasts to a range of BAPN concentrations to evaluate their temporal proliferation response and the expression of genes related to collagen synthesis and crosslinking, and to investigate the influence of mechanical loading on properties impacted by BAPN treatment. It was hypothesized that: (1) LOX and related genes would be upregulated by BAPN exposure to compensate for the reduction in enzymatic crosslinking; (2) osteoblast proliferation would have a dose-dependent negative response to BAPN exposure; (3) reduced crosslinking would alter the elastic properties of type I collagen; and (4) mechanical loading would beneficially influence properties impacted by BAPN treatment.

Materials and Methods

Cell culture

Calvarial osteoblasts were chosen for this study for their similarity to periosteal osteoblasts which experience substrate strain induced by mechanical loading. MC3T3-E1 Subclone 4 (ATCC® CRL-2593) murine preosteoblasts were obtained from the American Type Culture Collection (ATCC, Manassas, VA) and cultured in proliferation medium composed of α minimal essential medium (α-MEM, Life Technologies, Carlsbad, CA), 10% fetal bovine serum (FBS, GIBCO, Carlsbad, CA), 0.5% penicillin/streptomycin (GIBCO, Carlsbad, CA), and 1% L-glutamine (Hyclone, Logan, UT). MC3T3-E1 differentiation control medium consisted of proliferation medium supplemented with 50μg/mL ascorbic acid 2-phosphate (Sigma Aldrich, St. Louis, MO). Differentiation medium was also supplemented with BAPN (Sigma Aldrich, St. Louis, MO) for crosslink inhibition experiments.

BAPN dosage study

Quantitative reverse transcription polymerase chain reaction (qRT-PCR)—Cells were seeded into six polystyrene 6-well plates (500,000 cells per well), one of them a control plate without BAPN and the remaining five each treated with 0.25, 1, 2, 5, or 10mM BAPN (n=5 per group). Media was changed every 2–3 days. At the end of a 7 day differentiation period, the medium was removed from each culture dish and replaced with 1mL of TRIzol reagent (Invitrogen, CA). RNA isolation was performed using TRIzol reagent and reverse transcription (RT) was carried out using a High Capacity cDNA Reverse Transcription Kit (Life Technologies, Carlsbad, CA). PCR was performed using an ABI 7500 Fast PCR machine with SYBR Green primers using the Standard cycling mode modified for the PowerUp SYBR Green PCR master mix (Life Technologies, Carlsbad, CA). Primers were chosen for target genes encoding type I collagen α1 (*COL1A1*), type I collagen α2 (*COL1A2*), *LOX*, *BMP-1*, *POST*, as well as reference gene 18s RNA (*18S*) (Table 1) [24].

Each sample/gene combination was run in triplicate and water was used as the no-template control. mRNA expression levels of the triplicates were averaged. Following an efficiency-calibrated mathematical model [25], mRNA expression levels for each sample/target gene were averaged and compared to the control group using the REST® program [26]. The program calculates relative expression ratios using Equation 1 and employs randomization tests to obtain a level of significance.

$$Ratio = \frac{(E_{Target})^{\Delta CT_{Target}(Control-Sample)}}{(E_{Ref})^{\Delta CT_{Ref}(Control-Sample)}} \quad (1)$$

E_{Target} and E_{Ref} are the qRT-PCR efficiencies of a target gene and reference gene transcript, respectively; and ΔCT is the difference in control and sample cycle thresholds for the respective gene transcript.

Cell proliferation assay—Cells were seeded into three 96-well plates (5,000 cells per well), corresponding to BAPN treatment periods of 24, 48, and 72 hours. Within each plate, cells were seeded into 8 columns, one of them with control wells and the remaining seven each treated with with 0.125, 0.25, 0.5, 1, 2, 5, or 10mM BAPN (n=5 per group). The CellTiter 96® AQ_{ueous} One Solution Cell Proliferation Assay (Promega, Madison, WI) was used as a colorimetric method to determine the number of viable cells after BAPN treatment periods of 24, 48, or 72 hours. At the end of each treatment period, 20μL of CellTiter 96® One Solution Reagent was added to each well according to manufacturer instructions and the plate was incubated for 2 hours. The absorbance was then read at 490nm using an ELx800 microplate reader (BioTek, Winooski, VT) to measure the soluble formazan produced from the cellular reduction of the reagent's tetrazolium compound, a measurement directly proportional to the number of living cells in culture.

Mechanical loading study

The results from the dose-dependent study informed the mechanical loading experiments and a concentration of 2.0 mM BAPN was chosen for the remainder of the experiments. All cells were seeded into BioFlex® 6-well culture plates coated with fibronectin (ProNectin) to enhance adhesion, and cultured in the presence or absence of BAPN. After seeding, the proliferation medium was replaced with differentiation medium to promote collagen synthesis. A total of four groups cultured simultaneously were considered for this study to investigate the effects of BAPN treatment and mechanical loading: control-static, control-load, BAPN-static, BAPN-load.

Loading regimen—The BioFlex® plates were specially designed to respond to cyclic substrate strain *in vitro* applied by a Flexcell® FX-4000 computer-regulated vacuum pressure strain unit (Flexcell® International Corp., Burlington, NC). The unit applied a defined and controlled mechanical strain to samples in the control-load and BAPN-load groups by using sinusoidal negative vacuum pressure to deform the cell substrate. Control-static and BAPN-static samples were simultaneously cultured in the same incubator and adjacent to the strain unit during the loading period.

Cells were cyclically loaded to 5% elongation at 3 cycles/min (10 seconds strain, 10 seconds relaxation; 0.2Hz frequency) continuously for 7 days with a pause at day 3 to change media. It is worth noting that a circular loading post (25mm in diameter) was used to apply tension to the cell culture well which has been shown to result in biaxial strain across the surface directly over the post and a relatively large radial strain in the region in contact with the outer edge of the post [27]. One 7 day loading experiment was run per assay for this investigation and the manufacturer-recommended drying regimen was run between each 7 day loading period.

qRT-PCR—Cells were seeded into four 6-well Bioflex® plates (one plate per experimental group) at a density of 80,000 cells per well. Cells were cultured with or without mechanical loading in differentiation media, with or without BAPN supplementation. Differentiation medium was made by supplementing media with 50μg/mL ascorbic acid 2-phosphate (Sigma Aldrich, St. Louis, MO). Gene expression analysis was carried out as described previously.

Fourier Transform Infrared Spectroscopy (FTIR)—Using the same experimental methods described above, another experiment was performed to analyze the secondary structure of type I collagen using FTIR. Cells were seeded into four BioFlex plates, as described in the qRT-PCR methods above, and cultured in differentiation media with or without BAPN. Following 7 days of mechanical loading, the plates were cultured for 21 additional days under static conditions to allow time for collagen deposition and maturation. In preparation for FTIR data collection, media was removed and plates were rinsed four times with sterile milli-Q water. Samples were left hydrated overnight to allow the matrix to lift off of the substrate. Matrix samples were carefully transferred from their wells to barium fluoride windows using a cell scraper and rubber-coated tweezers, and air-dried.

FTIR spectroscopic analysis was performed using a Nicolet iN 10 infrared microscope (Thermo Fisher Scientific, Waltham, MA). A water vapor background was collected and subtracted from sample data as they were acquired. Data were collected from the samples at room temperature at a spectral resolution of $4cm^{-1}$. The amide I and amide II regions (~1400–1800cm^{-1}) were baseline corrected according to published standards [28–29] using OriginPro 2018 (OriginLab, Northampton, MA). Second derivative analysis was used to resolve underlying peaks within these regions and each spectrum was curvefit with Gaussian peaks using GRAMS/AI (Thermo Fisher Scientific, Waltham, MA). The results from the converged peak fitting were expressed as peak position, percentage area of the peak relative to the area underneath the fitted curve, and peak height. This investigation focused on peaks corresponding to positions at ~1660cm^{-1} and ~1690cm^{-1}, shown to be correlated to mature (HP, hydroxylysylpyridinoline) and immature crosslinks, respectively [22–23], [30–31].

Atomic force microscopy (AFM)-based indentation—In order to analyze elasticity of the type I collagen matrix, cells were seeded in four BioFlex plates as described in the qRT-PCR methods above. The loaded groups were loaded as described earlier for a period of 7 days. The cells were then cultured for an additional 7 days under static conditions and in differentiation medium prior to data collection. Prior to indentation, one well/sample per group was prepared by rinsing three times with phosphate-buffered saline (PBS). At this

point the PBS was aspirated and the well's silicone membrane was cut out using a disposable scalpel blade and carefully transferred to a 60mm petri dish. PBS was then added to the 60mm dish in order to keep the sample hydrated during indentation. After one sample from each group was indented, another set of samples from each group was prepared.

Multiple locations within each dish were indented in fluid and at room temperature (~24°C) with a Bioscope Catalyst AFM (Bruker, Santa Barbara, CA) in contact mode using a single calibrated bead AFM probe (Novascan Technologies, Boone, IA). This gold-coated silicon nitride probe had an attached borosilicate glass bead (5μm in diameter and spring constant of 0.065N/m). Before indenting, the probe was pushed onto a glass surface and the cantilever deflection was used to measure the probe's deflection sensitivity (nm/V). The AFM is mounted on a Leica DMI3000 inverted microscope (Leica Biosystems Inc., Buffalo Grove, IL) which allowed collagenous areas of interest to be identified. Indentations were made to a trigger force of 1nN at a speed of 0.5Hz and force-separation curves were acquired. On average, 7–10 areas were indented per sample for a total of 22–39 indents per group. A linear baseline correction was applied to the retraction curve and the reduced elastic modulus was fit for each unloading curve for roughly 15% to 70% of the maximum force using the Hertz model of elastic contact as reported by our group elsewhere[32].

Statistical analysis

BAPN dosage

Differences in mRNA expression between control and BAPN-treated samples were assessed for statistical significance in group means by using a Pair Wise Fixed Allocation Random Test©in the REST® program.

The cell proliferation absorbances were tested for a main effect of BAPN dosage using a one-way ANOVA for each time point followed by Dunnett's multiple comparisons test using GraphPad Prism version 7.04 for Windows (GraphPad Software, La Jolla, CA). A value of $p<0.05$ was considered significant for all experiments.

Mechanical loading

Differences in mRNA expression between control-static samples and each of the other three groups (control-load, BAPN-static, BAPN-load) were assessed for stastistical significance using the REST® program as described above.

The amide I peak area ratios, peak height ratios, and peak heights were tested for main effects of BAPN treatment and mechanical loading using a two-way ANOVA followed by a Tukey multiple comparisons test using GraphPad Prism version 7.04 for Windows (GraphPad Software, La Jolla, CA).

Anderson-Darling tests were used to detect indentation modulus distribution differences between each group.

Results

BAPN dosage study

qRT-PCR of cellular gene expression—Significant upregulation of *BMP-1*, *POST*, *COL1A1*, *COL1A2* was observed with exposure to various BAPN concentrations. Significant upregulation was noted at all concentrations for *BMP-1*, concentrations greater than 0.25mM for *POST*, and 1.0mM, 2.0mM, and 10.0mM BAPN for *COL1A1* and *COL1A2* (Table 2). *LOX* was upregulated at 1.0, 5.0, and 10.0mM though not to a statistically significant degree.

Cell proliferation assay—The cell proliferation results showed a trend of increased proliferation with increasing BAPN concentration at all three time points followed by a decline in proliferation at 10.0mM. The decline in proliferation was more pronounced at the 48 and 72 hour time points (Fig. 2).

After 24 hours of exposure to BAPN, a significant increase in proliferation relative to the 0mM BAPN control was found for 1mM ($p=0.0240$), 2mM ($p=0.0095$), and 5mM ($p=0.0231$) concentrations. The same was true for 5.0mM BAPN ($p=0.0276$) at the 48 hour time point, and for 0.25mM ($p=0.0315$) and 1.0mM ($p=0.0218$) at the 72 hour time point.

Mechanical loading study

Gene expression analysis—All mRNA expression data were analyzed with respect to the control-static group. *LOX* was significantly downregulated in the BAPN-load group with respect to the control-static group ($p=0.019$). *BMP-1* was significantly increased with BAPN treatment when comparing BAPN-static and control-static groups ($p=0.029$, Table 3).

Amide I crosslinking from FTIR spectra

Areas of interest for crosslinking analysis were identified using the infrared microscope and data were acquired from a minimum of five locations per sample. These five spectra were fit for underlying peaks and the results averaged to equal an n of 1 per sample. Spectra were collected from as many samples as possible though challenges arose during sample preparation and some samples became suboptimal for data collection. This resulted in sample size variation among groups: control-static, n=6; control-load, n=4; BAPN-static, n=6; BAPN-load, n=5. Peak fitting in the amide I region resulted in consistent peaks around $1661cm^{-1}$ and $1688cm^{-1}$ and were considered to be representative of HP and immature crosslinks, respectively.

Statistical analysis found a significant interaction between treatment and loading ($p=0.0244$) for the 1660:1690 peak area ratio (data not shown). Post-hoc analysis showed a significant increase in control-load versus control-static samples ($p=0.0188$). An interaction was also found for the $1660cm^{-1}$ peak area ($p=0.0014$) and post-hoc analysis found a significant increase in control-load relative to control-static samples ($p=0.0132$), and a decrease in BAPN-load compared to control-load samples ($p=0.0163$). In analyzing the ratio between amide I peak heights, a significant interaction was also detected ($p=0.0006$). Post-hoc

analyses indicated a significant increase in both control-load (p=0.0135) and BAPN-static (p=0.0012) samples compared to control-static samples (Fig. 3).

While a treatment-load interaction was discovered during analysis of the 1660cm^{-1} and 1690cm^{-1} peak heights (p=0.0074), the post-hoc test did not reveal any significant differences in peak height comparisons across groups. However, there was a trend towards an increased 1660cm^{-1} peak height in the control-load group compared to the control-static group (p=0.0827).

Elastic modulus from AFM indentation

Indentation was performed in each sample at as many locations as possible but identifying areas and acquiring indentation data from BAPN samples proved more challenging than with control groups. This was likely due to a difference in adhesion due to the presence of BAPN, and led to differences in sample size and number of indents: control-static, n=5; control-load, n=4; BAPN-static, n=4; BAPN-load, n=3. The BAPN-static group was found to have the highest mean indentation modulus at 0.251 ± 0.031kPa and BAPN caused a significant increase relative to control-load samples at 0.239 ± 0.032kPa (p=0.0499, Fig. 4). Mechanically loaded control samples had a mean modulus value of 0.216 ± 0.025kPa, which trended downward relative to static control samples resulting in a population distribution shift toward lower modulus values (p=0.0882, Fig. 5). There was no discernible difference between control-static and BAPN-load groups (0.231 ± 0.011kPa).

Discussion

It was hypothesized that *LOX* and other genes relating to collagen synthesis would be upregulated with increasing BAPN dosage to compensate for the reduction in enzymatic crosslinking. Results confirmed this hypothesis for multiple genes across a range of BAPN concentrations. *BMP-1*, *POST*, *COL1A1* and *COL1A2* were upregulated at most dosage levels greater than 0.25mM consistent with findings elsewhere [23], *POST* expression specifically increased in a dose-dependent manner. *LOX* remained unaffected even at 10.0mM BAPN which was roughly 70x higher than the ~0.137mM BAPN concentration used in prior *in vitro* studies showing changes in collagen morphology and crosslinking[20]. This indicates that factors other than *LOX* expression regulated the structural changes in response to BAPN noted in that study. It appears that *POST* upregulation in the presence of BAPN could have influenced *BMP-1*, as part of the LOX activation process. However, Maruhashi *et al.* revealed no significant difference in *BMP-1* expression between wild type (WT) and periostin$^{-/-}$ calvarial osteoblasts [13]. This supports the theory that BAPN exposure rather than the *POST* upregulation, was the driving force for *BMP-1* regulation in the present study.

These regulatory effects on *BMP-1* expression may have caused the difference in extracellular availability of activated LOX versus the pro-LOX precursor responsible for the structural and biochemical changes reported previously [20]. Low levels of BAPN (0.25 mM) in the present study caused significant upregulation of *BMP-1* relative to control, suggesting a compensatory effect to increase BMP-1-mediated processing of pro-LOX in response to BAPN exposure. This effect is substantiated by the significant upregulation of

type I collagen genes, *COL1A1* and *COL1A2*, in the presence of BAPN. The lowest BAPN concentration in this study was roughly twice that previously used[20], so further work would help determine whether the changes in collagen morphology and crosslinking occur regardless of any compensatory mechanism.

The second hypothesis of this study predicted osteoblast proliferation would have a dose-dependent negative response to BAPN exposure. The opposite effect was observed: proliferation increased with BAPN concentration and declined at the highest concentration of 10.0mM, particularly after 48 and 72 hours. These observations were not statistically significant relative to 0mM controls, which aligns with low BAPN dose results found by Fernandes et al [21]. Data collection was also limited to a culture period of three days at the end of which proliferation trended downward, particularly at the highest concentration. MC3T3-E1 cells are known to actively replicate during the initial development phase between 1 and 9 days of culture[33] which suggests the possibility of a temporary effect caused by BAPN-mediated upregulation of early osteogenic genes not considered in this study. The absence of a negative impact of BAPN on cell proliferation supports the more complex mechanism-driven theory alluded to earlier in the discussion of gene expression changes in response to BAPN treatment. More in-depth analysis of dose-dependent relationships between different BAPN dosages could help elucidate some of the underlying complexity of the mechanisms involved.

The gene expression findings coupled with the cell proliferation data encouraged exploration of how these effects translate to type I collagen protein properties at concentrations higher than those previously investigated [20]. The gene expression data suggested the greatest changes in collagen-related genes, namely *BMP-1, POST, COL1A1*, and *COL1A2*, occur with exposure to 1.0, 2.0, or 10.0mM BAPN. Cell proliferation data cautioned against exposure to 10.0mM BAPN for risk of a continued decrease in cellular metabolic activity with longer culture periods required for type I collagen accumulation. For these reasons, a BAPN concentration of 2.0mM was chosen for the mechanical loading characterization experiments.

In the mechanical loading experiments, BAPN was expected to upregulate *BMP-1*, *POST*, *COL1A1*, and *COL1A2* in accordance with results from the dose-dependent BAPN study. This trend was seen when comparing the BAPN-static group to the control-static group, though upregulation of *BMP-1* was the only significant outcome. This *BMP-1* upregulation with BAPN exposure supports a compensatory mechanism to increase conversion of the pro-LOX precursor to its active LOX form capable of initiating enzymatic crosslinking. *BMP*-1 was also upregulated by loading in both control and BAPN groups, though not significantly. Loading did, however, appear to mitigate the effect of BAPN on *BMP-1* expression, as evidenced by the lack of an effect in the BAPN-load group. The effect of loading was also present in the significant downregulation of *LOX* with BAPN treatment relative to static controls, as it caused a more pronounced effect than its BAPN-static counterpart. Loading alone was not found to regulate LOX because no differences in mRNA expression were seen between control-load and control-static samples. The downregulation of *LOX*, under loaded conditions, suggests that the strain experienced by the osteoblasts negatively impacted the availability of the LOX precursor, thereby limiting the availability of activated LOX and the

potential for enzymatic crosslinking. The focus of this study was on *LOX* and future studies would benefit from exploring these trends in other members of the family of LOX and LOXL genes as well.

Second derivative analysis of the type I collagen FTIR spectra revealed underlying peaks corresponding to mature (HP) and immature crosslinks. Treatment with BAPN increased the mature/immature peak height ratio in static samples, consistent with similar findings elsewhere [22], and caused a decline in HP peak area in loaded samples. This BAPN-mediated decline in mature crosslinking was consistent with a past study [20] although in loaded conditions of this study rather than static conditions. Taking both of these cases together, BAPN inhibition of enzymatic crosslinking via LOX inhibition was confirmed by the decrease in the peak area corresponding to mature crosslink HP, regardless of mechanical loading. Part of the hypothesis was that mechanical loading would influence properties impacted by BAPN treatment and loading was found to increase the mature/immature peak area ratio in control samples, a change driven by a significant increase in the HP peak area. Loading also appeared to mitigate the effects seen in BAPN-control samples. Under normal circumstances (absent BAPN LOX inhibition), mechanical loading has a positive influence on enzymatic crosslinking verified through increases in the HP peak area, mature/immature area ratio, and mitigative effects on BAPN inhibition.

To further evaluate the effect of mechanical loading on collagen properties impacted by BAPN treatment, BAPN-mediated inhibition of collagen crosslinking was assessed for its potential to affect the elastic properties of type I collagen. An upward trend in elastic modulus for BAPN samples compared to controls was revealed along with a significant increase in modulus in BAPN-static conditions relative to control-load conditions. Because of the interaction between both BAPN and loading, interpretation of the influence of either effect would benefit from further exploration. However, we can conclude that BAPN did not have a similar significant effect on modulus under loaded conditions which suggests loading has a mitigative effect on BAPN-mediated changes to elastic modulus. While BAPN did not have a clear broad effect on collagen elasticity, it impacted enzymatic crosslinking as noted earlier, suggesting that crosslinking along the length of the collagen fibril may not be as influential to the transverse elastic modulus measured using AFM-based indentation in this study. Furthermore, the indentation data showed a downward trend in modulus for loaded samples compared to static samples suggesting the cyclic strain applied to the cell substrate began to hinder formation of a stabilized collagen matrix. While the change was not significant, the proposed mechanism is substantiated by the observed decrease in LOX discussed earlier.

As with any two-dimensional cell culture model of any cellular environment, including that of osteoblasts, the model used in this study is unable to fully capture the complexity of its three-dimensional counterpart, much less the hierarchical intricacies of *in vivo* bone formation. For this reason, the investigation was approached from a mechanistic perspective to elucidate the effect of enzymatic crosslink disruption on collagen properties and explore mechanical loading via subtrate strain for potential compensatory effects.

In conclusion, BAPN treatment resulted in significant upregulation of genes involved in the enzymatic crosslinking process, a dose-dependent response in osteoblast proliferation, and an upward trend in collagen elasticity, while mechanical loading was found to mitigate its effects, particularly relating to *BMP-1* expression, mature/immature peak height, and elastic modulus. Future experiments might consider a decreased applied substrate stretch, modified loading frequency, a decreased loading period, or less constant loading with rest periods incorporated.

Acknowledgments

The authors are grateful to the IU School of Medicine Department of Anatomy & Cell Biology, particularly Dr. William Thopmson, for providing access to the Flexcell system and laboratory space, as well as Donna Roskowski in the IUPUI Department of Chemistry and Chemical Biology for providing access to the Nicolet iN 10 infrared microscope. This work was supported by funding from the NIH (AR072609, AR067221) and the authors wish to confirm that there are no potential conflicts of interest with respect to the authorship and/or publication of this article.

References

1. Burr DB, Allen MR (2013) Basic and Applied Bone Biology, 1st ed. Elsevier, San Diego, CA
2. Boskey AL, Wright T, Blank R (1999) Collagen and bone strength. J bone Miner Res 14:330–335 [PubMed: 10027897]
3. Burr DB (2002) The contribution of the organic matrix to bone's material properties. Bone 31:8–11. doi: 10.1016/S8756-3282(02)00815-3 [PubMed: 12110405]
4. Viguet-Carrin S, Garnero P, Delmas PD (2006) The role of collagen in bone strength. Osteoporos Int 17:319–36. doi: 10.1007/s00198-005-2035-9 [PubMed: 16341622]
5. Avery NC, Sims TJ, Bailey AJ (2009) Quantitative determination of collagen cross-links. Methods Mol Niology 522:103–21. doi: 10.1007/978-1-59745-413-1_6
6. Eyre DR, Paz M, Gallop P (1984) Cross-linking in collagen and elastin. Annu Rev Biochem 53:717–48. doi: 10.1146/annurev.bi.53.070184.003441 [PubMed: 6148038]
7. Eyre DR, Wu J-J (2005) Collagen Cross-Links. Top Curr Chem 247:207–229. doi: 10.1007/b103828
8. Saito M, Marumo K (2010) Collagen cross-links as a determinant of bone quality: a possible explanation for bone fragility in aging, osteoporosis, and diabetes mellitus. Osteoporos Int 21:195–214. doi: 10.1007/s00198-009-1066-z [PubMed: 19760059]
9. Dasler W (1954) Isolation of toxic crystals from sweet peas (Lathyrus odoratus). Science (80-) 120:307–308
10. Nimni ME (1977) Mechanism of inhibition of collagen crosslinking by penicillamine. Proc R Soc Med 70 Suppl 3:65–72 [PubMed: 122677]
11. Peng J, Jiang Z, Qin G, Huang Q, Li Y, Jiao Z, Zhang F, Li Z, Zhang J, Lu Y, Liu X, Liu J (2007) Impact of activity space on the reproductive behaviour of giant panda (Ailuropoda melanoleuca) in captivity. Appl Anim Behav Sci 104:151–161. doi: 10.1016/j.applanim.2006.04.029
12. Norris RA, Damon B, Mironov V, Kasyanov V, Ramamurthi A, Moreno-Rodriguez R, Trusk T, Potts JD, Goodwin RL, Davis J, Hoffman S, Wen X, Sugi Y, Kern CB, Mjaatvedt CH, Turner DK, Oka T, Conway SJ, Molkentin JD, Forgacs G, Markwald RR (2007) Periostin regulates collagen fibrillogenesis and the biomechanical properties of connective tissues. J Cell Biochem 101:695–711. doi: 10.1002/jcb.21224 [PubMed: 17226767]
13. Maruhashi T, Kii I, Saito M, Kudo A (2010) Interaction between Periostin and BMP-1 Promotes Proteolytic Activation of Lysyl Oxidase. J Biol Chem 285:13294–13303. doi: 10.1074/jbc.M109.088864 [PubMed: 20181949]
14. Fogelgren B, Polgár N, Szauter KM, Újfaludi Z, Laczkó R, Fong KS, Csiszar K (2005) Cellular Fibronectin Binds to Lysyl Oxidase with High Affinity and Is Critical for Its Proteolytic Activation. J Biol Chem 280:24690–24697. doi: 10.1074/jbc.M412979200 [PubMed: 15843371]

15. Turner CH, Pavalko FM (1998) Mechanotransduction and functional response of the skeleton to physical stress: The mechanisms and mechanics of bone adaptation. J Orthop Sci 3:346–355. doi: 10.1007/s007760050064 [PubMed: 9811988]
16. Ward DF, Salasznyk RM, Klees RF, Backiel J, Agius P, Bennett K, Boskey A, Plopper GE (2007) Mechanical strain enhances extracellular matrix-induced gene focusing and promotes osteogenic differentiation of human mesenchymal stem cells through an extracellular-related kinase-dependent pathway. Stem Cells Dev 16:467–80. doi: 10.1089/scd.2007.0034 [PubMed: 17610377]
17. Warden SJ, Galley MR, Hurd AL, Wallace JM, Gallant M a, Richard JS, George L a (2013) Elevated mechanical loading when young provides lifelong benefits to cortical bone properties in female rats independent of a surgically induced menopause. Endocrinology 154:3178–87. doi: 10.1210/en.2013-1227 [PubMed: 23782938]
18. McNerny EM, Gong B, Morris MD, Kohn DH (2015) Bone fracture toughness and strength correlate with collagen cross-link maturity in a dose-controlled lathyrism mouse model. J Bone Miner Res 30:455–464. doi: 10.1002/jbmr.2356 [PubMed: 25213475]
19. Hammond MA, Wallace JM (2015) Exercise prevents β-aminopropionitrile-induced morphological changes to type I collagen in murine bone. Bonekey Rep 4:645. doi: 10.1038/bonekey.2015.12 [PubMed: 25798234]
20. Canelón SP, Wallace JM (2016) β-Aminopropionitrile-Induced Reduction in Enzymatic Crosslinking Causes In Vitro Changes in Collagen Morphology and Molecular Composition. PLoS One 11:1–13. doi: 10.1371/journal.pone.0166392
21. Fernandes H (2009) The role of collagen crosslinking in differentiation of human mesenchymal stem cells and MC3T3-E1 cells. Tissue Eng Part A 15:
22. Thaler R, Spitzer S, Rumpler M, Fratzl-Zelman N, Klaushofer K, Paschalis E, Varga F (2010) Differential effects of homocysteine and beta aminopropionitrile on preosteoblastic MC3T3-E1 cells. Bone 46:703–709. doi: 10.1016/j.bone.2009.10.038 [PubMed: 19895920]
23. Turecek C, Fratzl-Zelman N, Rumpler M, Buchinger B, Spitzer S, Zoehrer R, Durchschlag E, Klaushofer K, Paschalis E, Varga F (2008) Collagen cross-linking influences osteoblastic differentiation. Calcif Tissue Int 82:392–400. doi: 10.1007/s00223-008-9136-3 [PubMed: 18488133]
24. Schmittgen TD, Zakrajsek BA (2000) Effect of experimental treatment on housekeeping gene expression: validation by real-time, quantitative RT-PCR. J Biochem Biophys Methods 46:69–81. doi: 10.1016/S0165-022X(00)00129-9 [PubMed: 11086195]
25. Pfaffl MW (2001) A new mathematical model for relative quantification in real-time RT-PCR. Nucleic Acids Res 29:45e–45. doi: 10.1093/nar/29.9.e45
26. Pfaffl MW, Horgan GW, Dempfle L (2002) Relative expression software tool (REST(C)) for group-wise comparison and statistical analysis of relative expression results in real-time PCR. Nucleic Acids Res 30:36e–36. doi: 10.1093/nar/30.9.e36
27. Vande Geest JP, Di Martino ES, Vorp DA (2004) An analysis of the complete strain field within Flexercell(TM) membranes. J Biomech 37:1923–1928. doi: 10.1016/j.jbiomech.2004.02.022 [PubMed: 15519600]
28. Yang H, Yang S, Kong J, Dong A, Yu S (2015) Obtaining information about protein secondary structures in aqueous solution using Fourier transform IR spectroscopy. Nat Protoc 10:382–396. doi: 10.1038/nprot.2015.024 [PubMed: 25654756]
29. Dong A, Huang P, Caughey WS (1990) Protein secondary structures in water from second-derivative amide I infrared spectra. Biochemistry 29:3303–3308. doi: 10.1021/bi00465a022 [PubMed: 2159334]
30. Paschalis E, Verdelis K, Doty SB, Boskey AL, Mendelsohn R, Yamauchi M (2001) Spectroscopic characterization of collagen cross-links in bone. J Bone Miner Res 16:1821–8. doi: 10.1359/jbmr.2001.16.10.1821 [PubMed: 11585346]
31. Paschalis E, Gamsjaeger S, Tatakis D, Hassler N, Robins S, Klaushofer K (2014) Fourier transform infrared spectroscopic characterization of mineralizing type I collagen enzymatic trivalent cross-links. Calcif Tissue Int 96:18–29. doi: 10.1007/s00223-014-9933-9 [PubMed: 25424977]
32. Kemp AD, Harding CC, Cabral WA, Marini JC, Wallace JM (2012) Effects of tissue hydration on nanoscale structural morphology and mechanics of individual Type I collagen fibrils in the Brtl

mouse model of Osteogenesis Imperfecta. J Struct Biol 180:428–38. doi: 10.1016/j.jsb.2012.09.012 [PubMed: 23041293]

33. Quarles LD, Yohay D a, Lever LW, Caton R, Wenstrup RJ (1992) Distinct proliferative and differentiated stages of murine MC3T3-E1 cells in culture: an in vitro model of osteoblast development. J bone Miner Res 7:683–92. doi: 10.1002/jbmr.5650070613 [PubMed: 1414487]

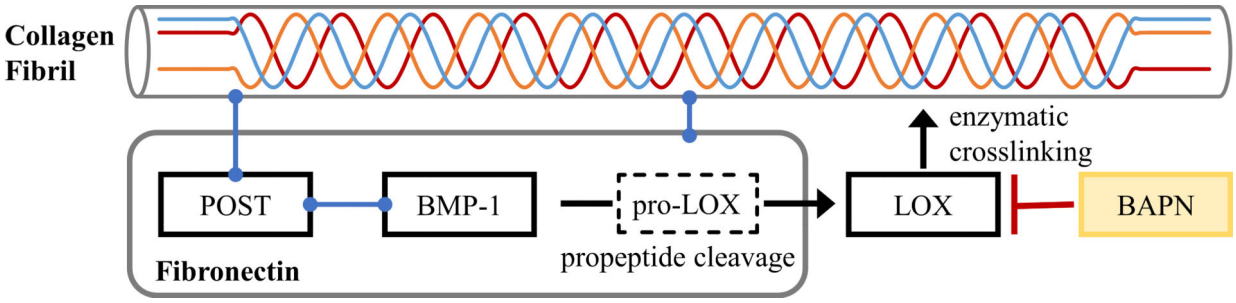

Figure 1.

Complex interactions impacting LOX activation and collagen crosslinking. LOX activation is dependent on POST and BMP-1 function and its activated form can be irreversibly bound by BAPN, preventing intra- and intermolecular enzymatic crosslink formation. Black boxes and arrows represent the process of LOX activation leading to enzymatic crosslink initiation, blue links represent binding between two components, and the red segment between LOX and BAPN represents the pair's inhibitory effect on crosslinking. POST, BMP-1, and pro-LOX all bind to fibronectin.

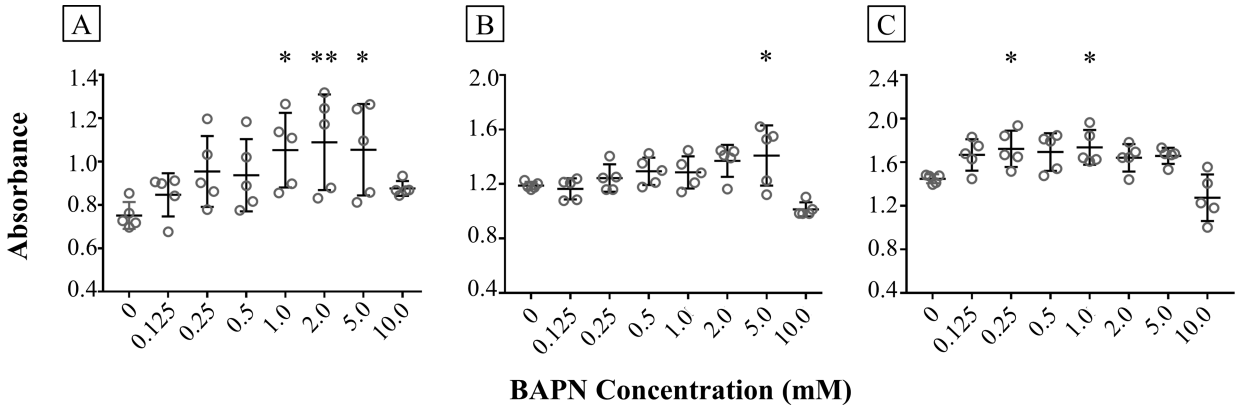

Figure 2.

Cell proliferation as a function of BAPN dosage (n=5). Proliferation after (a) 24 hours, (b) 48 hours, and (c) 72 hours. Statistically significant changes relative to 0mM BAPN controls indicated by * ($p<0.05$) and ** ($p<0.01$).

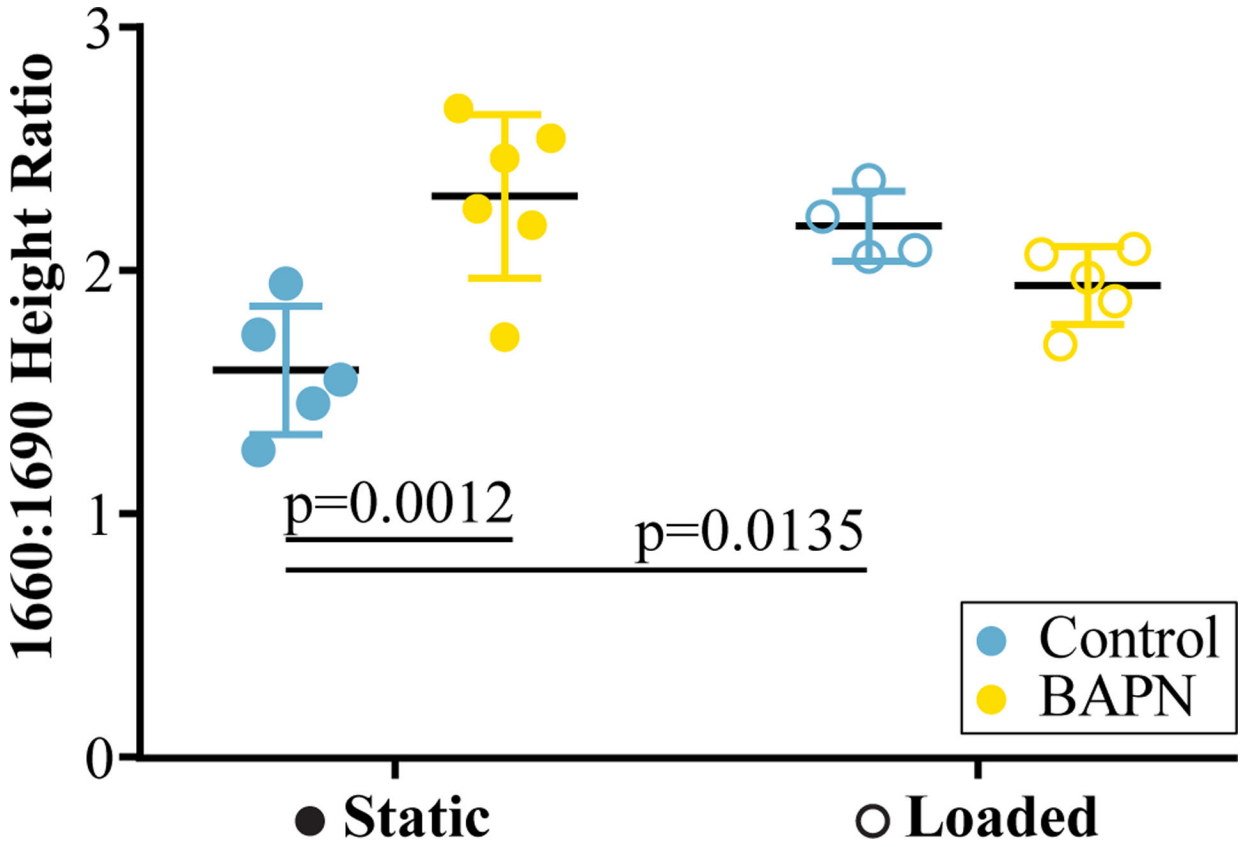

Figure 3.

Scatter plot of height ratio data (mean ± standard deviation). An increase in the ratio of 1660cm^{-1} to 1690cm^{-1} peak height is evident in control-static and BAPN-load relative to control-static. Significant differences are indicated by black bars between groups accompanied by p-values.

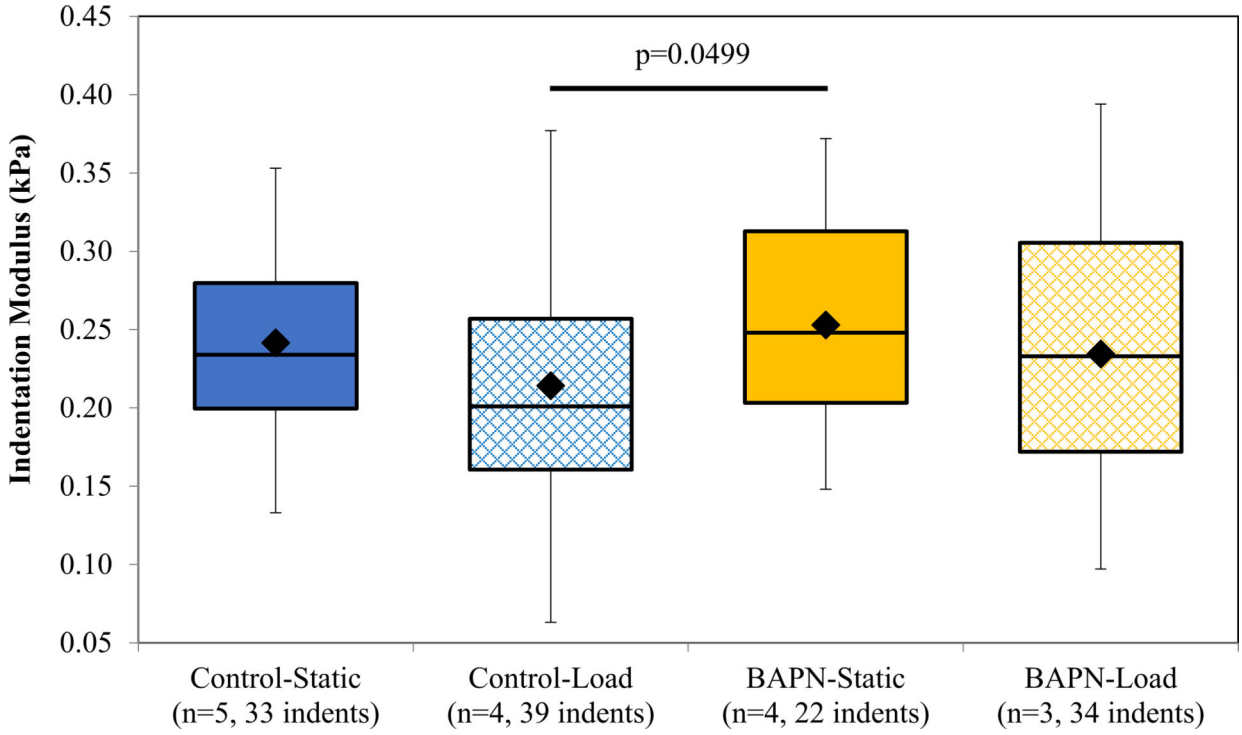

Figure 4.

Boxplot representation of the spread of indentation modulus data. An increase in mean indentation modulus is evident in the BAPN-static samples relative to control-load samples, as is the similarity between the control-static and BAPN-load groups. Mean values are marked by the diamond marks on the boxplots.

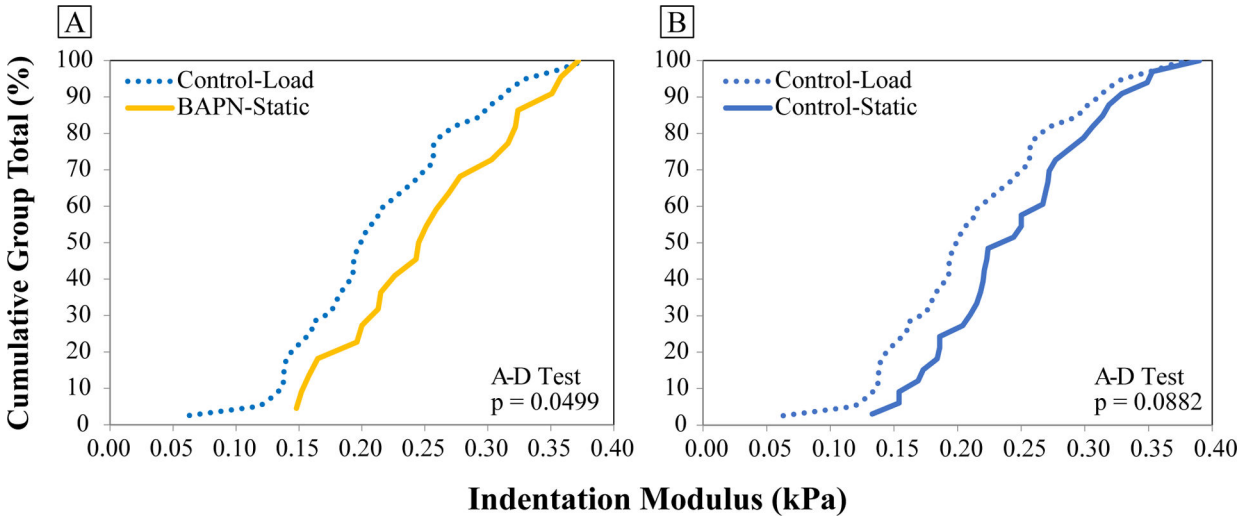

Figure 5.

Cumulative distribution function representation of indentation modulus data. There is a clear shift towards a (a) higher indentation modulus in the BAPN-static group relative to the control-load group and (b) lower indentation modulus in the control-load group relative to control-static.

Table 1:

Gene primer sequences.

Full Name	Forward Sequence (5' to 3')	Reverse Sequence (5' to 3')
Collagen Type I α1 (COL1A1)	GCAACAGTCGCTTCACCTACA	CAATGTCCAAGGGAGCCACAT
Collagen Type I α2 (COL1A2)	CAGAACATCACCTACCACTGCAA	TTCAACATCGTTGGAACCCTG
Lysyl Oxidase (LOX)	TACTCCAGACTCTGTGCGCT	GGACTCAGATCCCACGAAGG
Bone morphogenetic protein-1 (BMP-1)	CTTCCCTCAATCACCCAGACT	TAAAGATTAGGGACACCGGCTA
Periostin (POST)	GGAATTCGGCATTGTGGGAGCCACTACC	GGTCGACTCAAATTTGTGTCAGGACACGGTC
18s rRNA (18s)	GTAACCCGTTGAACCCCATT	CCATCCAATCGGTAGTAGCG

Table 2:

Fold changes in mRNA expression of BAPN-treated samples relative to controls.

Target Gene	0.25mM	1.0mM	2.0mM	5.0mM	10mM
LOX	0.737 (0.625 – 0.969)	1.138 (0.880 – 1.508)	0.934 (0.716 – 1.255)	1.402 (1.065 – 1.761)	1.469 (1.178 – 1.809)
BMP-1	2.072 (1.506 – 2.902)*	2.705 (2.120 – 3.529)*	2.622 (1.861 – 3.814)*	2.212 (1.700 – 2.992)*	2.299 (1.762 – 3.093)*
POST	1.207 (0.616 – 2.274)	3.443 (1.716 – 6.963)*	4.407 (2.165 – 8.833)*	6.058 (3.328 – 11.738)*	10.468 (5.079 – 20.207)*
COL1A1	1.327 (0.907 – 1.991)	1.835 (1.202 – 2.892)*	2.179 (1.495 – 3.448)*	1.724 (1.056 – 2.736)	1.897 (1.311 – 2.988)*
COL1A2	1.517 (0.967 – 2.189)	1.652 (1.096 – 2.462)*	1.944 (1.335 – 3.075)*	1.395 (0.871 – 2.421)	1.892 (1.239 – 2.892)*

Fold changes reported with 95% confidence interval (n=3 for LOX, n=5 for all other targets).

*Indicates statistically significant changes ($p<0.05$).

Table 3:

Fold changes in mRNA expression in all samples relative to the control-static group

Target Gene	Control-Load	BAPN-Static	BAPN-Load
LOX	0.743 (0.523 – 1.012)	0.707 (0.547 – 0.966)	0.593 (0.440 – 0.777)*
BMP-1	1.17 (0.915 – 1.437)	1.334 (1.053 – 1.626)*	1.264 (1.021 – 1.577)
POST	1.639 (1.029 – 2.664)	1.15 (0.725 – 1.661)	1.272 (0.774 – 2.249)
COL1A1	1.162 (1.055 – 1.398)	1.052 (0.908 – 1.243)	0.978 (0.832 – 1.164)
COL1A2	1.1 (0.899 – 1.301)	1 (0.812 – 1.221)	1.075 (0.867 – 1.414)

Fold changes reported with 95% confidence interval (n=4).

*Indicates statistically significant changes ($p<0.05$).